CANADIAN JOURNAL OF EXPLORATION GEOPHYSICS
VOL. 29, NO. 1 (JUNE 1993), P. 216-226

OBSERVATIONS OF ANISOTROPIC CUSPS IN TRANSVERSELY ISOTROPIC CLAY

COLIN SLATER[1], STUART CRAMPIN[1], LEONID Y. BRODOV[2] AND VASILIY M. KUZNETSOV[2]

ABSTRACT

Three-component seismograms from two shear-wave source orientations in eight walkaway VSPs to two wells in the Juravskoe Oil Field in the Caucasus Basin display anisotropic cusps. These are caused by strong transverse isotropy with a vertical axis of symmetry in a 1200 m-thick layer of uniform clay. The arrival times and polarizations of the shear waves, including the cuspidal arrivals, can be matched by full-wave synthetic seismograms in a model with the clay having transverse isotropy with 41% *qSH*-wave and 27% *qSV*-wave anisotropy. These appear to be the first published reports of anisotropic cusps in exploration seismics to be confirmed by matching with synthetic modelling. Techniques for exploring clay reservoirs have not yet been established and such cuspidal arrivals may be useful as they provide additional new signals with new properties for examining structures and tracing the *qSV* wavefront. These experiments are the first to use new techniques designed to optimize acquisition geometry for recording seismic anisotropy.

The experiments also show strong azimuthal variations of anisotropy (affecting source radiation, shear-wave source polarization, traveltime and wavelet shape), known as natural directivity (ND), in the top few hundred metres of the uniform horizontal structure.

INTRODUCTION

In 1991, Neftegeofizika Geolkom, Moscow, Stavropol-Neftegeofizika, Stavropol, and the Edinburgh Anisotropy Project, British Geological Survey, Edinburgh, collaborated in walkaway VSP experiments in two wells, Nos. 85 and 87, in a clay reservoir in the Juravskoe Oil Field in the Caucasus Basin of Russia. Such clay reservoirs are comparatively common in oil fields throughout the Russian Platform and western Siberia and are thought to be present in many areas elsewhere. Clay reservoirs are often characterized by production rates varying from hundreds of tons per day to zero over comparatively short distances. The reservoir we investigate is in the bottom 100 m of a 1200 m-thick layer of uniform clay, and the distribution, orientation and internal structure of the oil-bearing inclusions are clearly crucial to productivity. Techniques for exploring such reservoirs are not yet established, and the primary aim of the collaboration is to use shear waves and shear-wave splitting to extract information about the orientation and characteristics of the oil-filled inclusions in the clay reservoir layer (Brodov et al., 1992) where Well No. 85 is producing and Well No. 87 is not producing. This preliminary report analyzes anisotropic cusps observed in record sections of shear-wave walkaways through the thick clay layer above the reservoir.

The behaviour of shear-wave splitting and anisotropy varies with the azimuth and angle of incidence of the raypath in three dimensions. Consequently, the information about anisotropy that can be extracted from any particular experiment depends critically on the three-dimensional geometry of the source-to-geophone raypaths (Brodov et al., 1992). Depending on the structure and orientation of the anisotropic symmetry, particular record sections may or may not contain the information required, or may possibly duplicate information along other (expensively acquired) record sections. This makes it important to optimize acquisition geometry in relation to what is known about the geological structure and the stress directions and orientation of the anisotropy in order to maximize the information content at minimal cost. Making minimal assumptions about the form of the inclusions, the recording geometry for these VSP walkaways in the Caucasus was optimized using a data-based inversion scheme for anisotropic parameters (MacBeth et al., 1993). These are the first field experiments where acquisition geometry has been optimized for anisotropic information using this technique. Essential features of such geometry, as has long been recognized (Crampin, 1987), are walkaways in directions which are not parallel to the supposed symmetry (stress) directions and source orientations that generate both split shear-wave polarizations.

During the course of the experiment with the optimized geometry anomalously fast SV-wave arrivals were identified on all walkaway profiles and recognized as being caused by cusps. This paper confirms, by modelling with full-wave

'Department of Geology and Geophysics, University of Edinburgh, Grant Institute. West Mains Road. Edinburgh EH9 3JW; also, Edinburgh Anisotropy Project, British Geological Survey, Murchison House, West Mains Road, Edinburgh EH9 3LA

'Neftegeofizika Geolkom, Chemyshevsky Str.22, Moscow 10 1000

We thank Gareth Yardley and geophysicists from Neftegeofizika and Stavropol-Neftegeofizika for their contributions (and their good company) during the field work. Synthetic seismograms were calculated with the ANISEIS package of Applied Geophysical Software Inc., Houston and Macroc Ltd., Edinburgh. This research was supported by Neftegeofizika Geolkom, Stavropol-Neftegeofizika, the Sponsors of the Edinburgh Anisotropy Project and the Natural Environment Research Council and is published with the approval of the Director of the British Geological Survey (NERC).

synthetic seismograms, that these anomalous phases are generated by cusps on the SV-wave group-velocity surfaces caused by the high differential shear-wave anisotropy. Although cusps are well established theoretically, and are expected in strong anisotropy, there appears to be no reports synthetically modelling cusps in field observations before this study. Previously, Jolly (1956) observed abnormally large SV-wave velocities in field observations in (Pierre) shale and offered these, qualitatively, as observations of cusps. Later Levin (1979) presented an explanation of these observations in terms of general cusp arrival time behaviour and White (1982), although not discussing Jolly or Levin's work, shows results on cusp amplitudes which support Levin. The possible importance of exciting cuspidal arrivals for field studies is that they can provide additional signals along raypaths through zones of interest and place further constraints on interpretation of the fluid-filled inclusions without acquiring additional data sets. The terminology we use for describing anisotropy is that suggested by Crampin (1989).

TRANSVERSE ISOTROPY AND CUSPS

Velocities of both *P*- and S-waves propagating obliquely in sedimentary sequences may differ substantially from vertical velocities. This is characteristic of hexagonal anisotropic symmetry, that is transverse isotropy about a vertical symmetry axis leading to azimuthal isotropy. Uhrig and Van Melle (1955) report anisotropy factors as large as $K = 1.4$ for P-waves, where $K = V_{horiz}/V_{vert}$, and Brodov et al. (1984) report anisotropy factors for shear waves as large as $K = 1.5$. Brodov et al. note that most argillaceous sediments are transversely isotropic with clays having particularly pronounced shear-wave anisotropy.

Riznichenko (1949) and Postma (1955) showed that such effective transverse isotropy could be caused by (P)eriodic sequences of (T)hin isotropic (L)ayers (PTL anisotropy) with layer thicknesses smaller than the seismic wavelengths. Lithological anisotropy of aligned grains may also cause such transverse isotropy (Kaarsberg, 1968) and, since lithological anisotropy and PTL anisotropy have very similar patterns of elastic constants, it is difficult to separate the cause from their effects on seismic waves. Clays typically display little bedding and the observed transverse isotropy is believed to be caused by the lithology of preferentially aligned grains.

Musgrave (1954) showed theoretically that materials with strong transverse isotropy may have cusps in the SV-wave group-velocity surfaces, caused by the high curvature of the SV-wave phase-velocity variations. One of the clearest indications of cusps on record sections is anomalously fast arrivals. The only previous publication reporting observations of anisotropic cusps in exploration seismics appears to be Jolly (1956), interpreted by Levin (1979).

GEOLOGY OF JURAVSKOE OIL FIELD

Wells Nos. 85 and 87 are located in the foredeep, north of the Caucasus Mountains, 5 km and 10 km southwest of the village of Blagodamyy, 100 km east of Stavropol (Figure 1). The flat-lying geology, determined previously by well logs, seismic reflection and VSP surveys, consists of an almost horizontal sequence, about 600 m thick, of Neogene clays, sandstones and limestones overlying the Maikop Series of Middle Oligocene to Lower Miocene rocks (Nalivkin, 1973). The uppermost 200 m of the Maikop in the area of the wells is an alternating sequence of sandstones and clays overlying 1200 m of uniform clay with the reservoir in the lowest 100 m. The velocity structure in Figure 2a, derived from a near-offset VSP, indicates continuous clay below 870 m with a small gradient in P-wave velocity and a slightly larger gradient in shear-wave velocity, with V_p/V_s ratios between 2.1 and 3.0. High V_p/V_s ratios between 1.8 and 3.0 are characteristic of clay beds (Castagna et al., 1985). The increase of V_s and decrease in V_p/V_s below 1950 m in the clay reservoir is thought to be caused by the presence of organic-rich material in the clay.

DATA ACQUISITION

The walkaway profiles suggested by the acquisition optimization procedure (MacBeth et al., 1993) were two source polarizations along two azimuths with geophones at two levels in two cased vertical wells, Nos. 85 and 87. We examine the data set from Well No. 85 in this study but all walkaway profiles from both wells show similar features. The geophone levels spanned the 100 m-thick reservoir zone near the bottom of the 1200 m-thick clay layer of uniform clay. Figure 1 shows the layout of the acquisition geometry and Table 1 lists details of the field experiment at Well No. 85.

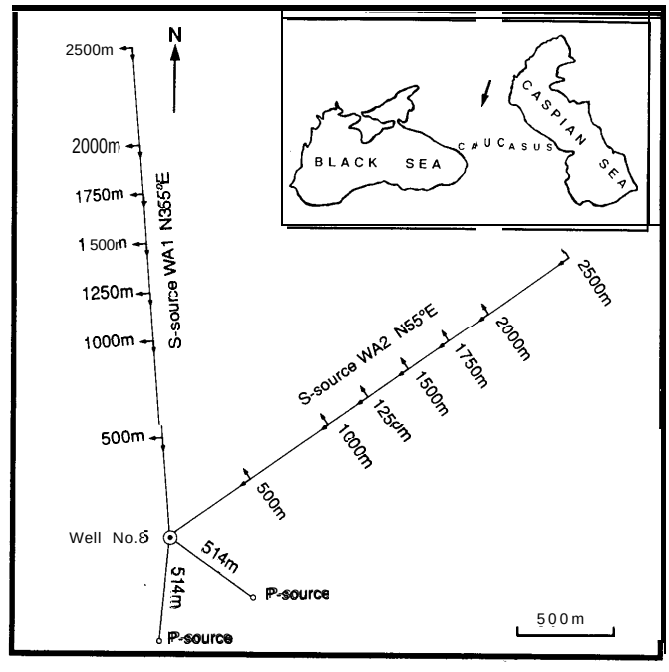

Fig. 1. Location of Caucasus region with arrow marking study area and acquisition geometry for Well No. 85 showing walkaway shear-wave offsets.

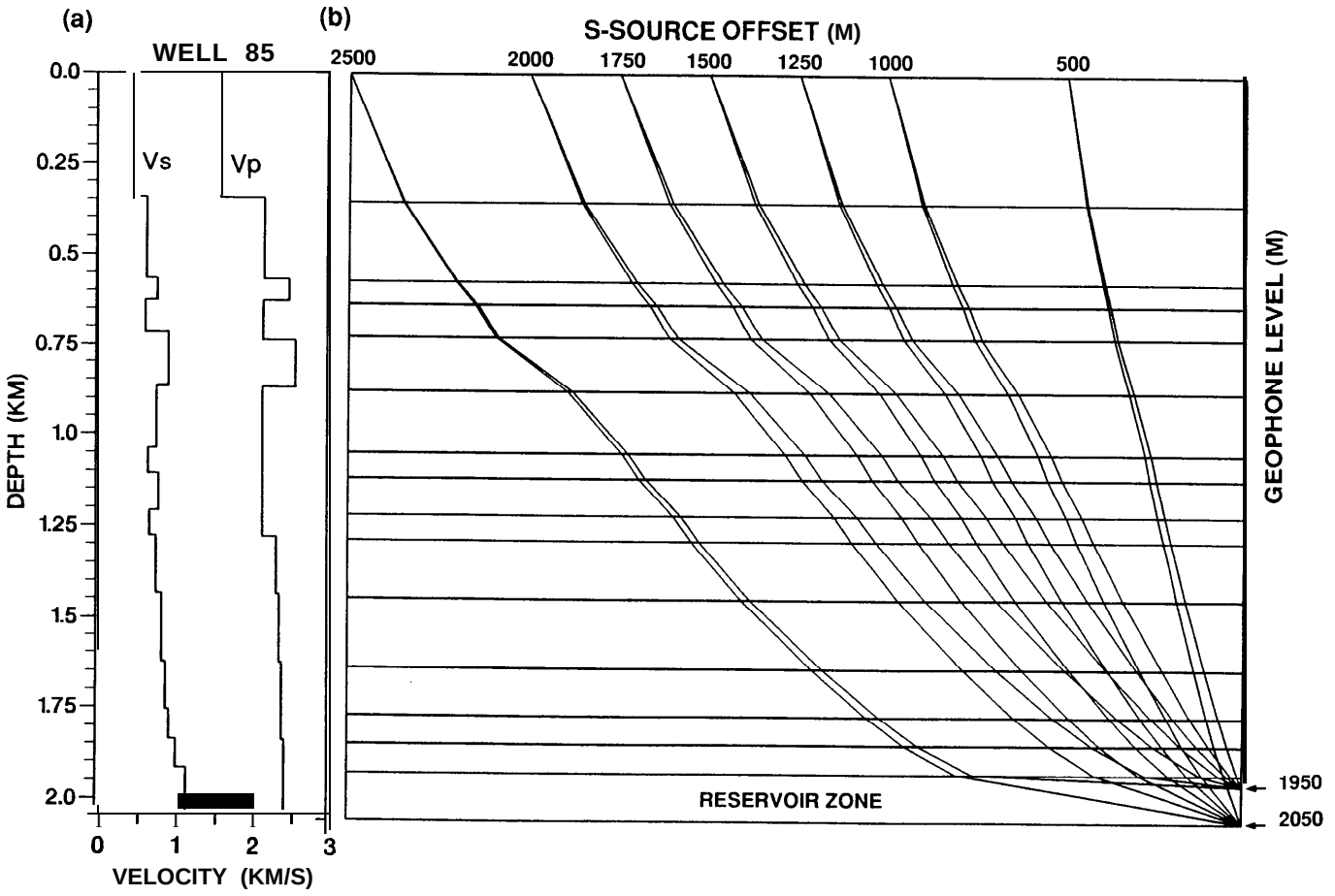

Fig. 2. **(a)** Isotropic velocity structure derived from a near-offset VSP, and **(b)** ray tracing shear waves through the isotropic velocity structure in (a).

Table 1. Details of the field experiment at Well No. 85.

EQUIPMENT AND LAYOUT	
S-wave source	Electrodynamic VEIP-40 truck
Peak frequency	16Hz
Offset from wellhead	500-2500 m
Azimuth of walkaways	1) N355°E, 2) N55°E
P-wave source	400-g blocks of explosive
Peak frequency	100 Hz
Offset from wellhead	514 m
Azimuth	1) N125°E, 2) N185°E
Geophone system	Orthogonal 3-component, moving coil
Geophone levels	1950 and 2050 m
Field filters	10 Hz low-cut, 50 Hz Notch
Sample rate	1 ms
Record length	6 s

Shear waves were generated with an impulsive electrodynamic source, the VEIP-40 (Table 1), aligned in-line and cross-line to the direction of the wellhead. Since the walkaways were not parallel to stress/symmetry directions such source orientations excited both split shear-wave polarizations. Each truck had three baseplates producing a horizontal force giving impulsive signals with, in this experiment, an effective centre frequency of 16 Hz. The source signals were stacked (up to 32 times for the widest offset with a 3200-m raypath) with left and right source polarizations at each geophone level allowing P-wave signals to be cancelled and shear-wave signals enhanced by subtracting seismograms of opposite source polarizations (Puzirev and Brodov, 1969). Correspondingly, *P-waves* were enhanced and shear waves cancelled by adding opposite polarizations. To determine orientations of the downwell geophones, high-energy *P*-waves were generated by explosives in shallow boreholes at offsets of 5 14 m.

ANALYSIS

Figure 3 shows three-component seismograms for two sources along two walkaways with the geophone at the 1950-m level in Well No. 85. (Note that the offsets along each walkaway are 250 m apart except for the first and last offsets which are 500 m apart.) Since the relative arrival times of phases on different components of the seismic traces, important for this study, are usually well separated displays of polarization diagrams (hodograms) are not informative. We prefer to display these walkaway records as three-component record sections (Figure 3), rather than four-, six- or nine-component matrix displays as has become conventional in

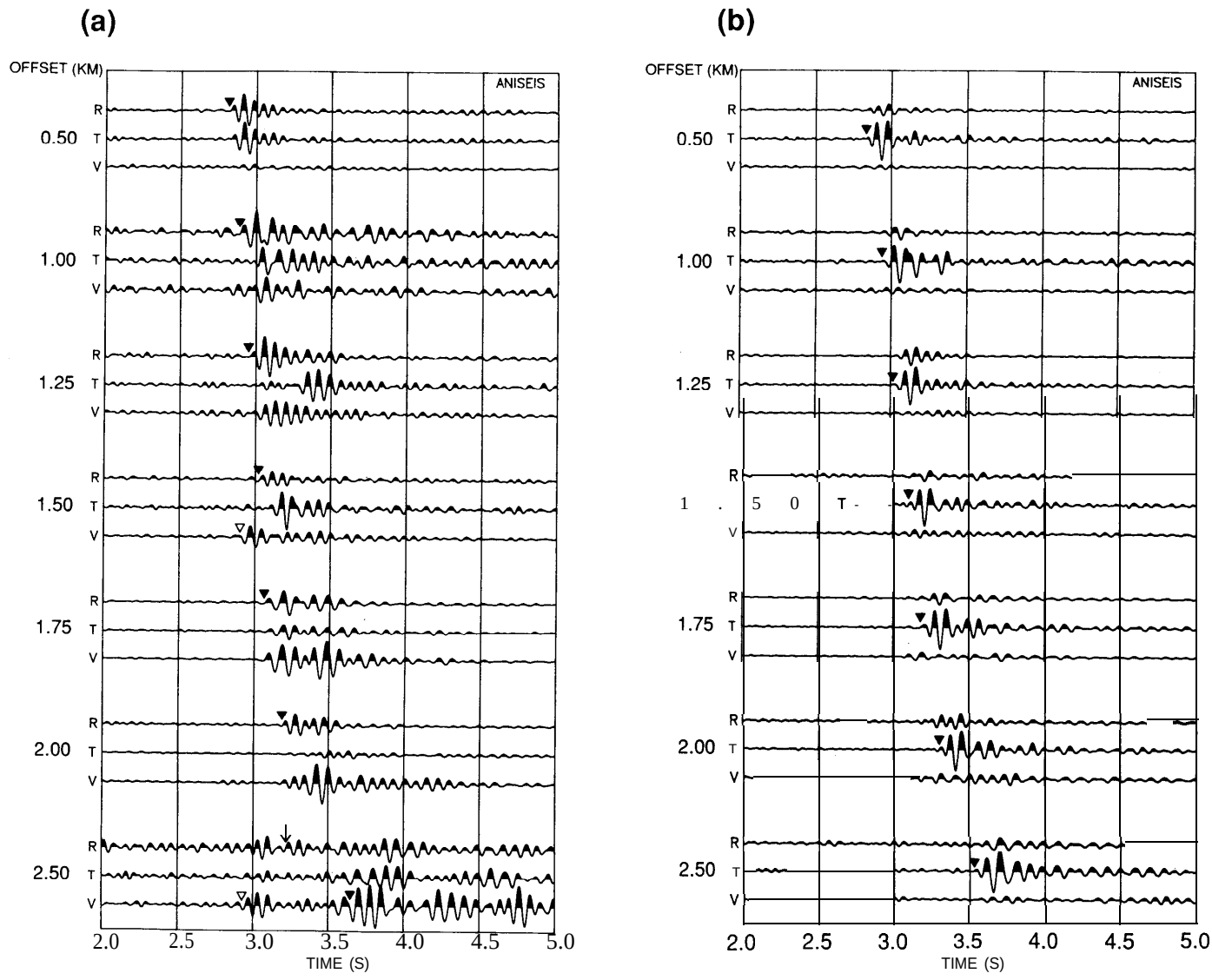

Fig. 3. Three-component seismograms recorded by geophone at 1950-m level for walkaway WA1 at an azimuth of N355°E for (a) in-line, and (b) cross-line source orientations and for walkaway WA2 at an azimuth of N55°E for (c) in-line, and (d) cross-line source. Seismograms are (V)ertical and horizontal (R)adial (in-line) and (T)ransverse (cross-line) and time is from origin. Each three-component seismogram is normalized separately. The small solid triangles mark arrival times of the main body-wave phases used to estimate the transverse isotropy and the open triangles mark anomalous arrivals which synthetic seismograms show are generated by a cusp (1500-m offset) and by a shallow P-to-S conversion (2500-m offset). The arrow (2500-m offset) marks an arrival which synthetic seismograms (Figure 7) show is also cuspidal.

displays of vector data sets where analysis of smaller time separations is required.

The data sets from the two walkaways show many similarities with the largest differences being between the relative amplitudes of the three-component signals. All eight walkaways show very similar features and most of the following comments and modelling results, including observations of cuspidal arrivals, apply equally to all walkaways. There are many anomalous features in Figure 3, particularly the multiple shear-wave arrivals with different velocities (leading to different arrival times) and different polarizations. These multiples have similar arrival times at the corresponding offsets and geophone levels along the different walkaways, but the relative three-component amplitudes vary substantially between offsets and geophone levels and between walkaways (compare the two walkaways in Figure 3).

The arrivals we attempt to model directly are the anomalous fast arrivals at the 1500-m and 2500-m offsets, marked by open triangles. These appear on record sections of both walkaways in Figure 3, and on all other walkaways to all geophone levels, as does the cross-coupling between arrivals on the sagittal plane and the transverse horizontal direction that would not be expected in a flat-layered isotropic or azimuthally isotropic structure. We match the field seismograms with synthetic seismograms by proceeding successively from isotropic models to transversely isotropic to azimuthally anisotropic models. The synthetic seismograms are computed by a reflectivity technique (Taylor, 1990).

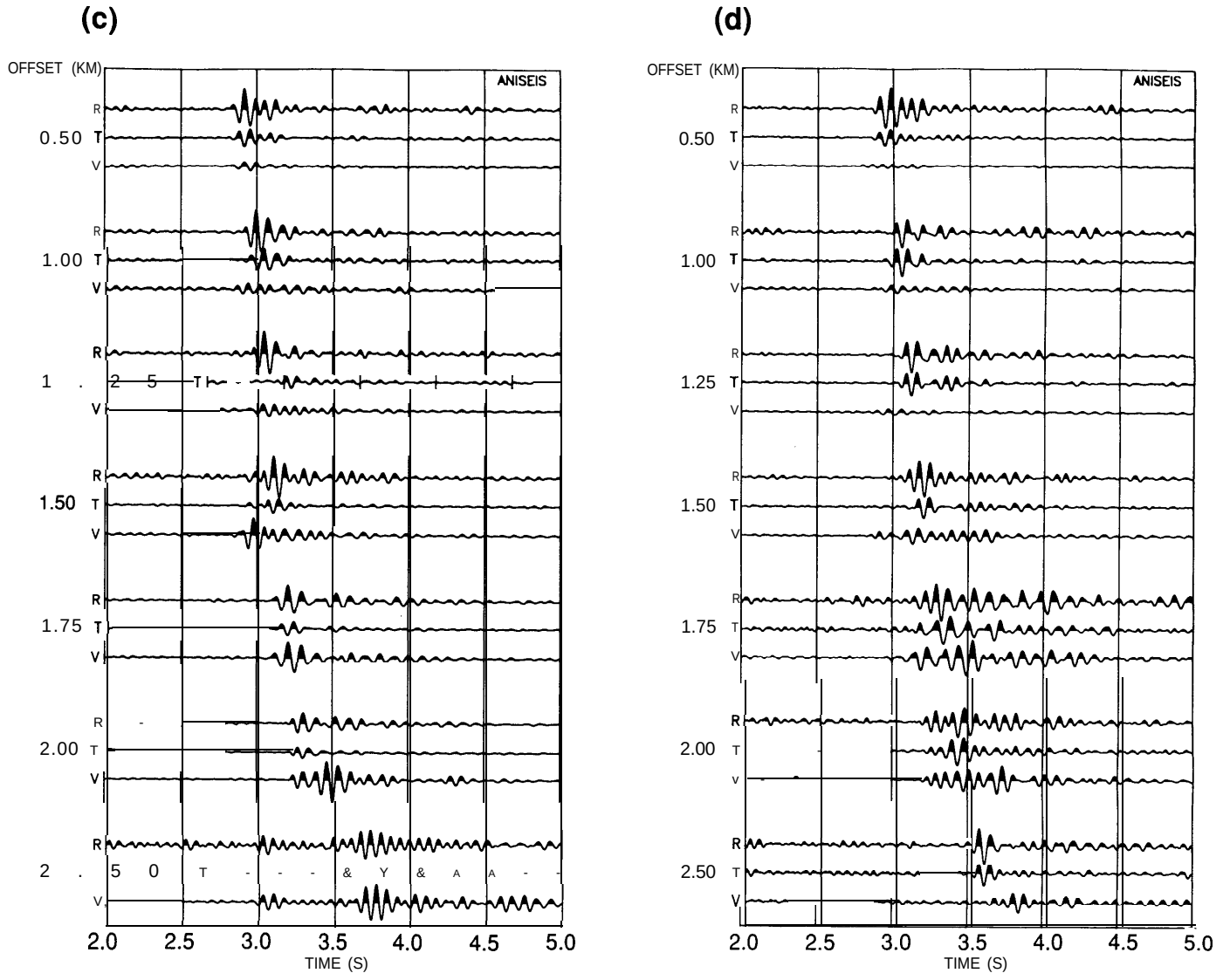

Fig. 3 (Cont'd).

Modelling raypaths in an isotropic structure

Figure 2a shows the isotropic velocity structure obtained from a near-offset VSP survey and Figure 2b shows shear-wave ray tracing from the walkaway offsets through this structure [density was derived from the algorithm of Gardener et al. (1974)]. Figure 4 shows the corresponding synthetic seismograms for in-line and cross-line source orientations to the 1950 m-level geophone. Substantial differences in arrival times between the field data in Figure 3 and the synthetic seismograms in Figure 4 show that, although the model gives appropriate arrival times for near-vertical propagation at the 500 m offset as would be expected, the differences in traveltime increase with offset to about 700 ms for the 2500 m offset. This indicates that horizontal velocities are substantially greater than vertical velocities which is characteristic of transversely isotropic structures.

Modelling raypaths in a transversely isotropic structure

The shear-wave ray tracing in Figure 2b shows that, except for the 2500 m offset, the raypaths are quite close to straight lines, particularly through the clay from 870 m to 1900 m. Although the incidence angles at the geophone are different from the isotropic raypaths in Figure 2b, the deviations of the raypaths are comparatively small and source-to-geophone straight lines are a good first-order approximation to the true raypaths. Arrival times were picked, as indicated by small solid triangles in Figures 3a and 3b. Figure 5a shows the estimated (group) velocity variations derived from these picks plotted against incidence angle assuming straight-line raypaths for walkaway WA1 in Figure 3. The estimated velocities for WA2 are almost identical. Extrapolation to the axes in Figure 5a suggests substantial transverse isotropy of about *34% qSH*-wave and 24% *qSV*-wave anisotropies and 19% P-wave velocity anisotropy.

For transverse isotropy, the square of the P-wave phase velocity is expected to have an approximately sin 28 variation with angle from the symmetry axis (with a, usually small, sin 48 contribution), and the squares of the *SH*- and SV-wave phase-velocity variations are similarly expected to have approximately sin 28 and sin 48 variations, respectively, where the coefficients of the sin 48 variations of the squares of *P*- and SV-wave phase velocities are equal and opposite in sign (Crampin, 1981). Seismic rays propagating at the group velocity, derived by differentiating the phase velocity, have more complicated surfaces, which may in some circumstances contain cusps. However, these simple geometric relationships are strictly valid at the axes (0" and 90°) where phase and group velocities are equal and provide simple inversion techniques for elastic constants.

Projecting the variations in Figure 5a to the axes at 0" and 90" provides four of the five elastic constants specifying a transversely isotropic solid. The fifth constant can be adjusted to match the details of the separation (in percent) between the two shear-wave group velocities. The elastic constants of this transversely isotropic model are listed in Table 2 and the velocity variations are shown in Figure 5b. The solid lines in the figure are the phase velocities showing the sin 28 and sin 48 variations. The dashed lines are the group velocities (joined to the appropriate phase velocity) where the *SV* curve displays the expected cusps. Estimated field group velocities are superimposed from Figure 5a and show a good match with the modelled group velocities. This model is used to provide a base from which to prepare further anisotropic models for the individual layers.

Since most of the transverse isotropy is expected to be in the clay interval (Brodov et al., 1984) from 870 m to 2050 m, a fifteen-layer model was made up containing 15% *SV*- and 18% SH-wave anisotropy in the layers above 870 m and 27%

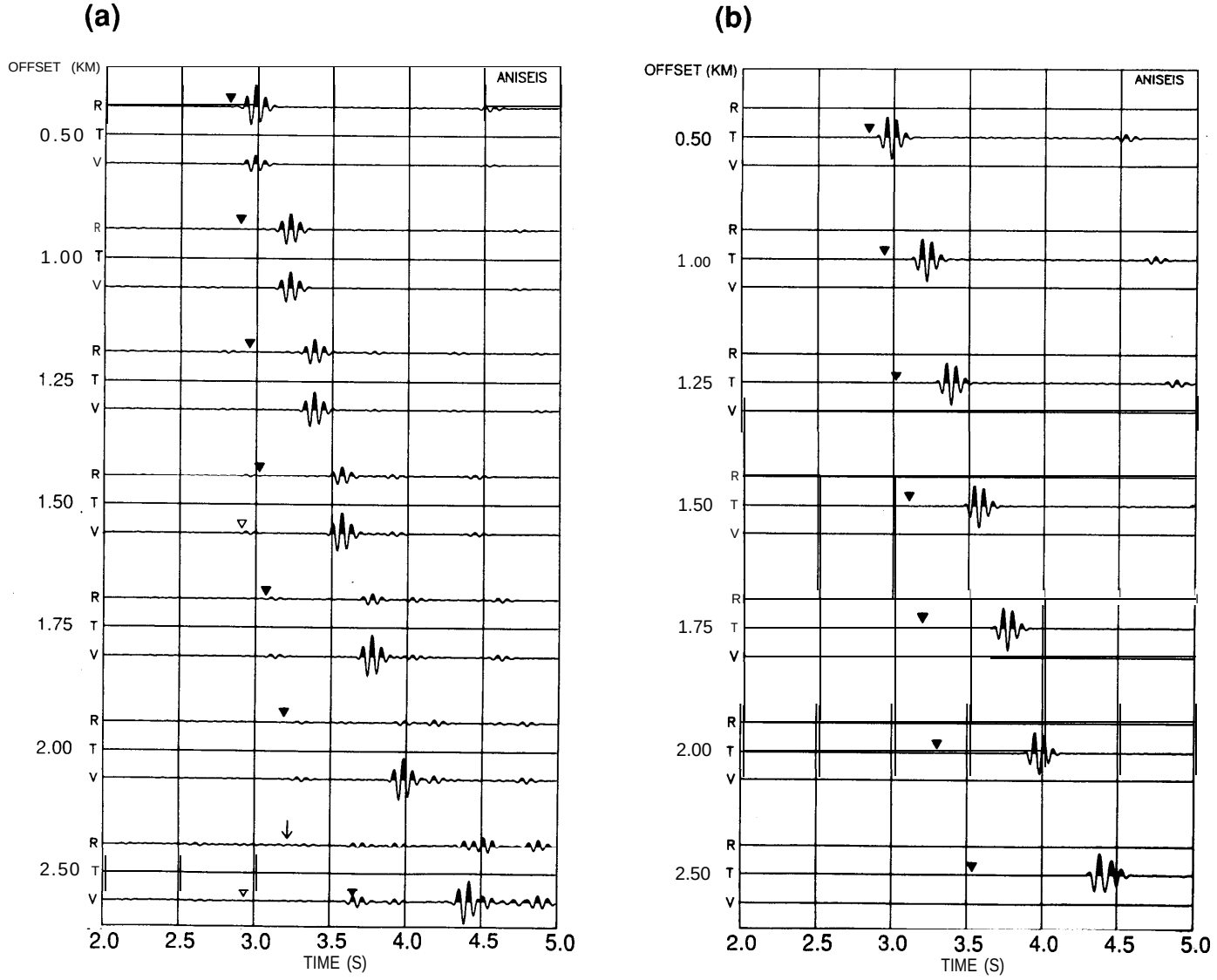

Fig. 4. Three-component synthetic seismograms for a walkaway survey to a geophone at 1950-m level through the multilayered isotropic structure in Figure 2a for (a) in-line, and (b) cross-line source orientations. Notation as in Figure 3.

SV- and 41% W-wave anisotropy in the clay layers below level 870 m . A program was written to insert given percentages of *P*- and shear-wave anisotropy in each layer, given the velocities along the vertical symmetry axis in Figure 2a. The fifth constant was adjusted to match the W-wave (and P-wave) sin 48 variations. Figure 5c shows the velocity variations through layer No. 9 with 41% *SH*- and 27% W-wave anisotropy in the anisotropic clay interval. There is a pronounced cusp. Figures 6a and 6b show synthetic seismograms calculated for in-line and cross-line source orientations for walkaways through this fifteen-layer transversely-isotropic model. Despite the relative simplicity of the modelling, most essential features of the field data in Figure 3 are reproduced, except for the variable sagittal to transverse coupling. The arrival times and amplitudes of all of the main phases are similar and, in particular, the arrival times and amplitudes of the anomalous phases at offsets of 1500 m and 2500 m marked by open triangles are similar. The anomalous phase at 1500 m offset is wholly determined by the cusp and is generated near the centre of the cusps in Figures 5b and 5c.

The first anomalous arrival at the 2500 m offset, marked by an open triangle in Figure 3a and matched by the synthetic seismograms, is the shear wave from a P-to-S conversion at the larger impedance contrasts above the top of the clay (above 870 m). There is a possible second anomalous arrival on the radial-component seismograms at 2500 m offset marked by an arrow. To demonstrate these arrivals in more detail, Figure 7 shows synthetic seismograms calculated for 100 m-interval offsets between 1000 and 2500 m in the transversely isotropic structure. The arrival just later than the arrow at the 2500 m offset can be traced directly to the cusp at 1500 m offset, showing that the arrival in Figure 3a is cuspidal. The cuspidal arrivals at the intervening 1750 m and 2000 m offsets are not sufficiently separated in time from the

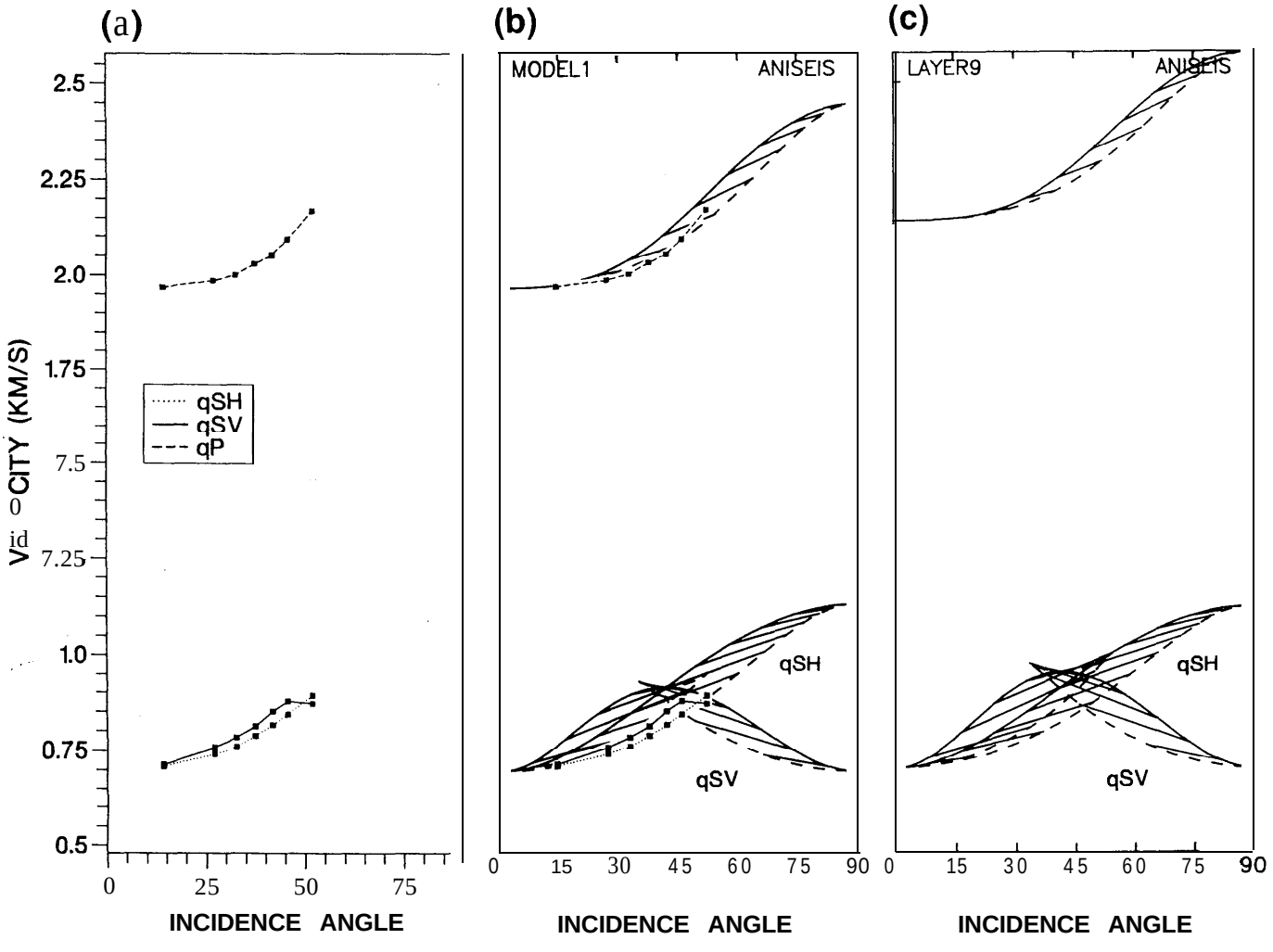

Fig. 5. (a) Velocities estimated from seismograms in Figures 3a and 3b assuming straight raypaths: dashed line is P-wave velocity variations; solid line is W-wave variations; and dotted line is *SH*-wave variations. (b) Velocities in the transversely isotropic model matching the estimated velocities in (a). Solid lines are phase velocities and dashed lines are group velocities joined to equivalent phase velocity by lines at every 10° of phase-velocity direction. The group velocities from the observations in (a) are superimposed in (b). (c) Velocities in transversely isotropic layer 9 with same notation as (b).

main shear-wave arrivals to be clearly identified in Figure 3, but the general form of the arrivals from the SV-source orientation are well reproduced by the synthetic seismograms in Figures 6a and 6b.

We suggest that these models confirm that anomalously fast arrivals at offsets of 1500 m and 2500 m are generated by cusps. However, a characteristic feature of the field records that is not modelled by the transversely isotropic model in Figures 6a and 6b is the coupling between motion in the sagittal (V-R) plane and the transverse (T) direction which is a dominant feature of the field seismograms in all eight walkaways. Such coupling between sagittal and transverse-horizontal directions is characteristic of the azimuthal anisotropy of aligned vertical cracks (Crampin and Lovell, 1991).

Table 2. Elastic constants in 10^9 Pa for straight raypaths in Figure 5b and Layer 9 in Figure 5c. Density is p = 2.11 g/cm^3.

ELASTIC CONSTANTS FOR FIGURE 5.					
	$c_{1111} = c_{2222}$	c_{3333}	c_{1122}	$c_{3311} = c_{2233}$	$c_{2323} = c_{3131}$
Figure 5b	12.585	8.155	7.178	6.550	1.019
Figure 5c	14.027	9.663	8.052	7.796	1.040

Modelling raypaths in an azimuthally anisotropic structure

The presence of azimuthal anisotropy must be invoked to model the sagittal to transverse coupling in the field data; however, a full discussion of the azimuthal anisotropy is beyond the scope of this paper. In summary, the near-offset VSPs at Wells Nos. 85 and 87, not shown here, both display evidence of strong but very different near-surface azimuthal anisotropy in a homogeneous flat "layer-cake" stratigraphy. Well No. 87 shows a 20-ms delay between split shear waves established by a depth of 300 m, whereas No. 85 shows insignificant splitting at 300 m. The field data in Figure 3

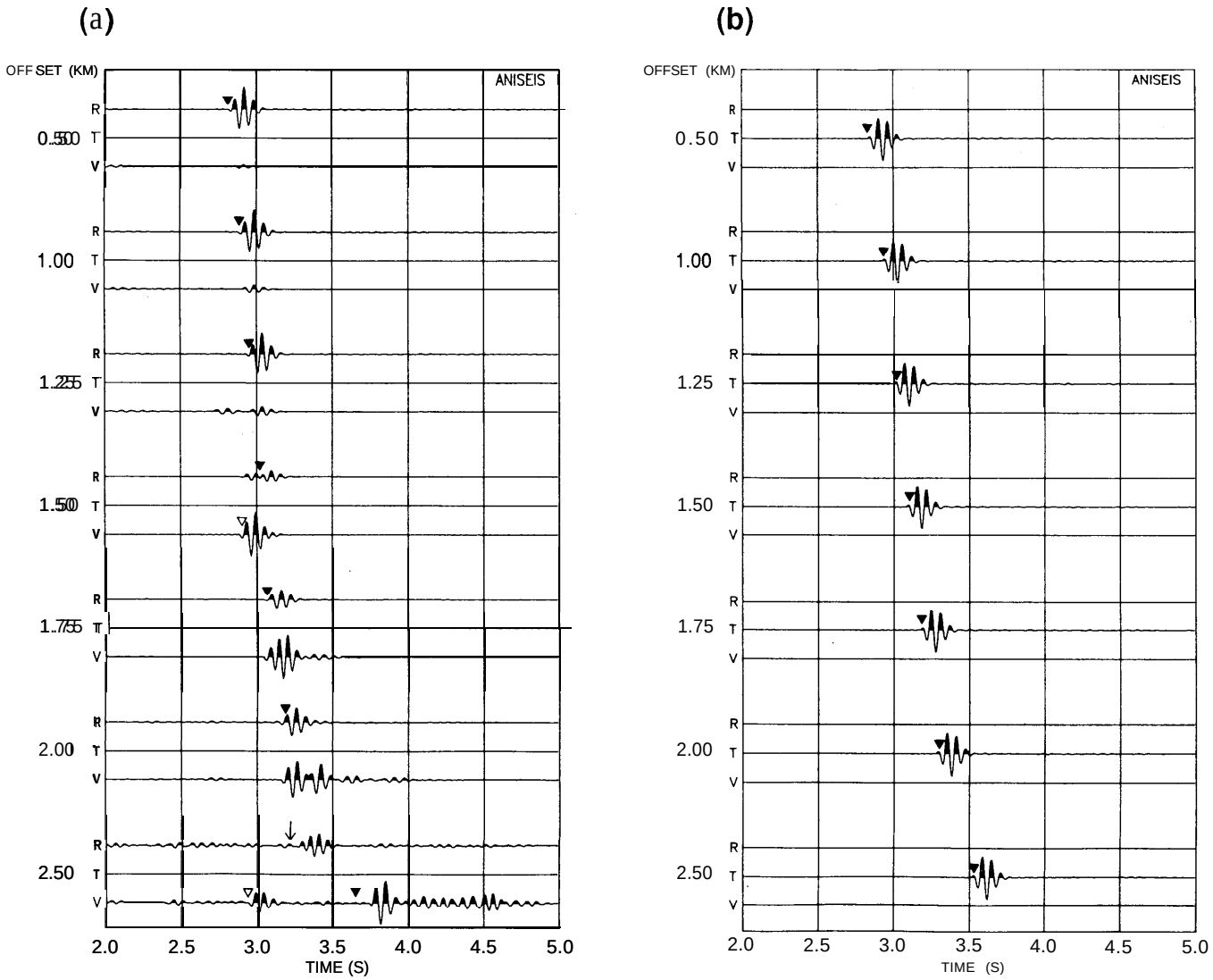

Fig. 6. Synthetic seismograms for a walkaway at azimuth N355°E modelling WA1 recorded with the geophone at the 1950 m level through the fifteen-layered transversely isotropic model for **(a)** in-line, and **(b)** cross-line source orientations.

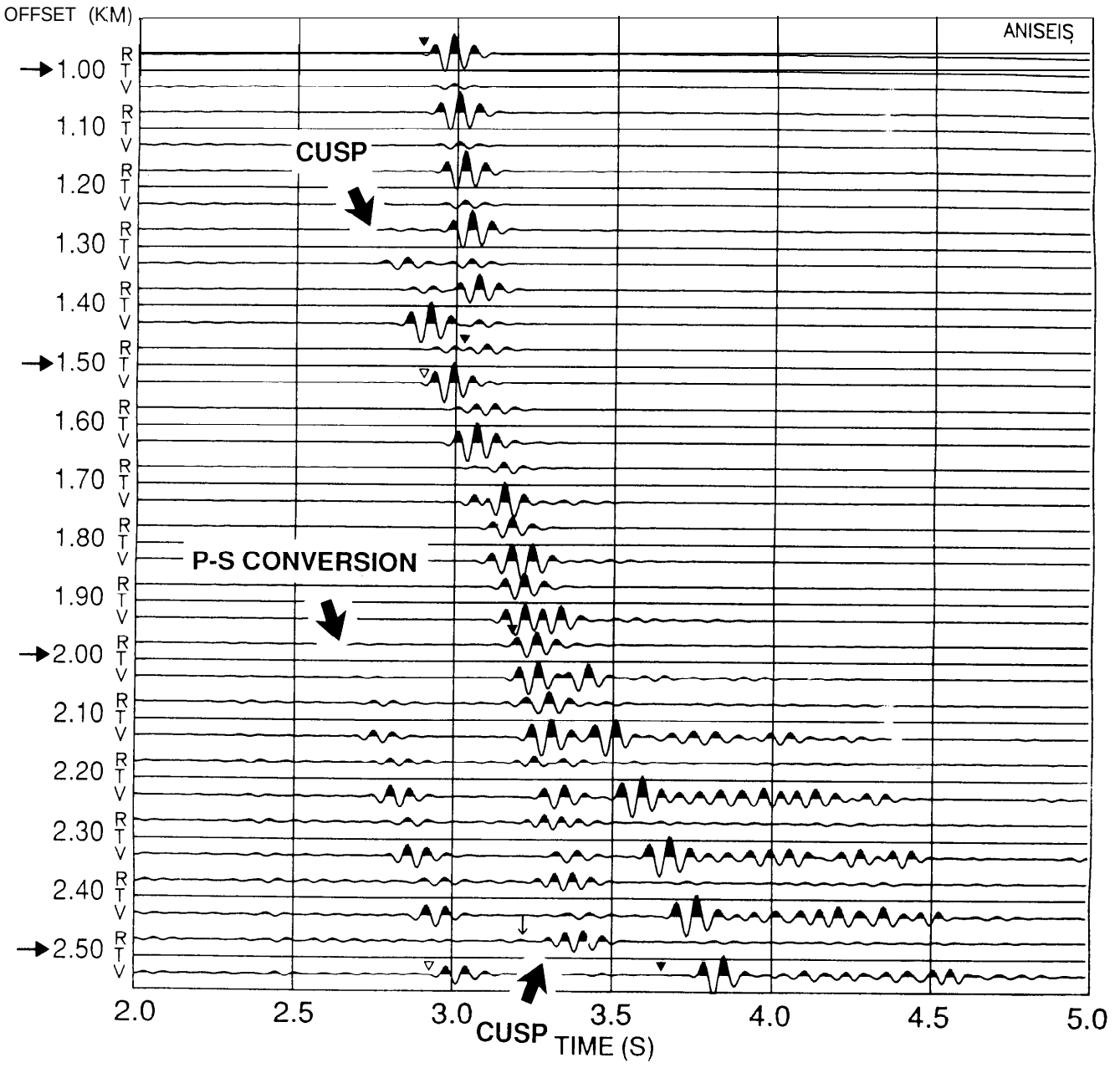

Fig. 7. Synthetic seismograms modelling WA1 (Figures 3a and 3b) from 1000-m offset to 2500-m offset at 100-m intervals, through the same transversely isotropic structure as Figure 6. Arrows in the left margin indicate offsets for which there are observations.

show strong coupling for near-vertical incidence at the 500 m offset. This can be modelled by introducing vertical cracks (Crampin and Lovell, 1991; Crampin, 1993) into the top 870 m with crack density $\varepsilon = 0.014$ and strike N203°E.

Figures 8a and 8b show synthetic seismograms through this orthorhombic structure for in-line and cross-line source orientations along an azimuth of N355°E modelling walkaway WA 1. Comparison with the field data in Figure 3 shows that all the previous similarities in the sagittal plane and the transverse motion are preserved and that many features of the coupling between the sagittal and transverse motion are also reproduced. In particular, some features of the multiple shear-wave arrivals with different arrival times and polarizations as well as reverberatory *P*- and shear-wave coda (which could easily be mistaken for instrumental noise) also appear in the synthetic seismograms in Figures 8a and 8b. However, many details are not explained, particularly the relative amplitudes of the three-component signals which sometimes vary substantially between offsets in Figure 3a and 3c. These anomalies appear to be near-surface effects at the various source offsets caused by a phenomenon known as natural directivity, which we describe below.

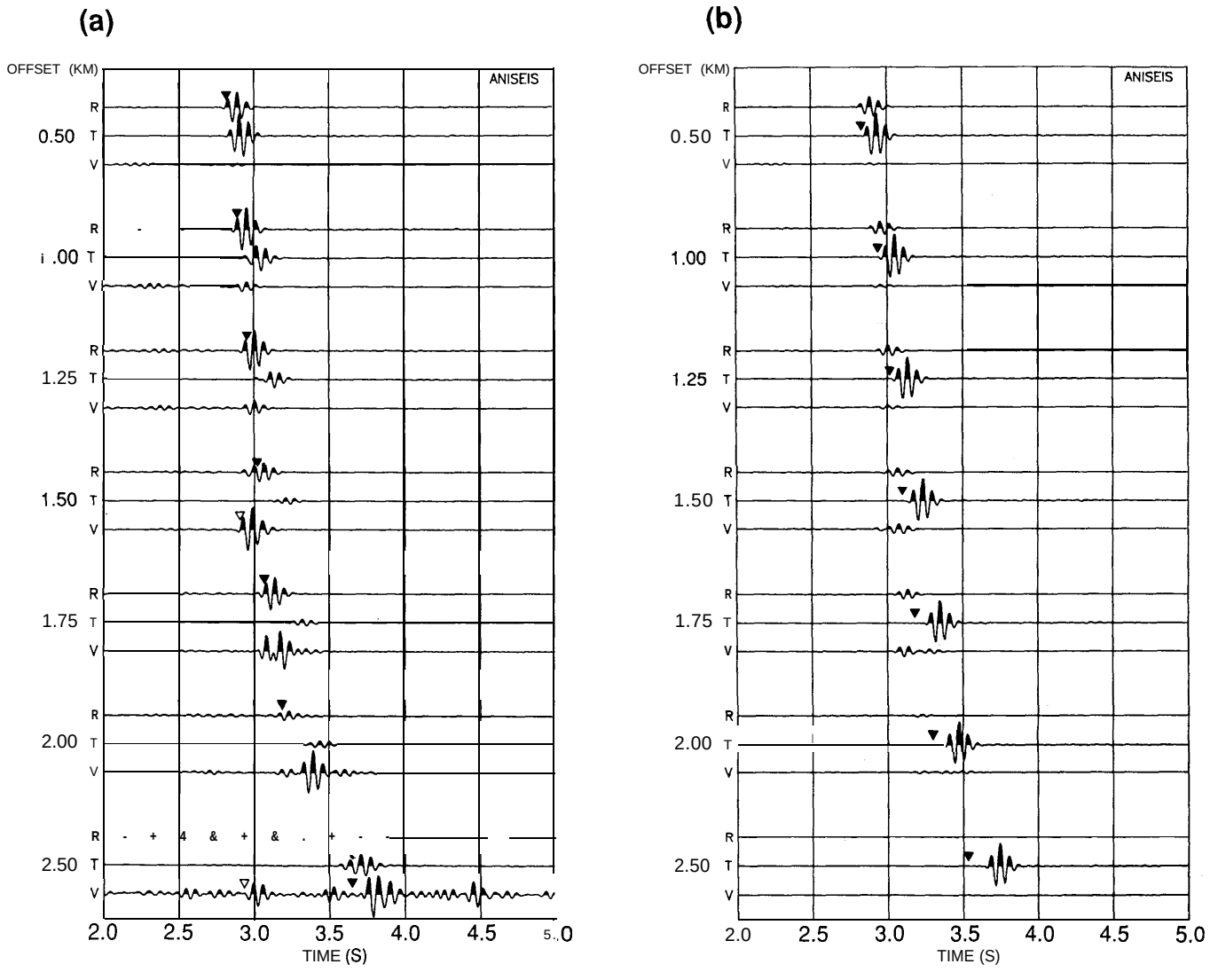

Fig. 8. Synthetic seismograms modelling WA1 (Figures 3a and 3b) through the same fifteen-layered model as in Figure 6, but now containing parallel vertical cracks in the layers above 870 m leading to azimuthal anisotropy for (a) in-line, and (b) cross-line source orientations.

NATURAL DIRECTIVITY

The presence of strong near-surface anomalies in shear-wave behaviour, particularly the nonorthogonality of radiation patterns from orthogonal shear-wave sources., has been recognized in Russia (Puzirev et al., 1985) where it is known as natural directivity (ND). It may result in unpredictable shear waves from explosions and anomalies in polarization and radiation from surface shear-wave sources. The causes of ND are not fully understood. Variations in ND can sometimes be correlated with varying consolidation in poorly consolidated sediments and may vary substantially over distances of metres (Puzirev et al., 1985). ND may also be caused by multiple reflections from inclined interfaces and near-surface bedding.

It is tempting to dismiss ND as shear-wave statics, in the same way as P-wave statics is usually dismissed as an uninteresting necessity. However, since details of waveforms are essential for interpreting shear waves correctly, identifying ND is essential for accurate evaluation of shear-wave behaviour. Pronounced delays between split shear waves (100 ms in 600 m) at a VSP experiment in the Geysers geothermal site in California were originally thought to be caused by the presence of parallel cracks (Majer et al., 1988). These large delays were actually caused by P-to-S conversions in an 11 m-thick isotropic surface layer with very low shear-wave velocity (Campden et al., 1990) and the large delays were independent of the crack geometry below the surface layer.

Since the effects of ND frequently display characteristic anisotropic features and can vary rapidly over short distances, it has implications for the detailed interpretation of ‘any shear-wave source deployed at the surface. Unless recognized, ND can complicate the interpretation of shear-wave reflection surveys and, as here, walkaway shear-wave VSPs, where it would be impracticable to make a detailed study of

the uppermost few hundred metres at each offset. We suggest that the irregularities of the relative amplitudes of three-component field data in Figure 3 were probably caused by variations in ND near each offset source location. The amplitudes of each three-component seismogram could be matched by varying the near-source structure, particularly the orientation of cracks, at the site of each shear-wave source.

CONCLUSIONS

To model arrival times of shear waves in the walkaway VSPs transverse isotropy with a vertical axis of symmetry was included, with 41% *SH*- and 27% SV-wave anisotropy in 1200 m-thick Maikop clay. Subsequently, anomalously fast arrivals, particularly the 200 ms early precursor at 1500-m offset, have been identified and matched with synthetic seismograms. These arrivals are generated at cusps in the *SV*-wave group-velocity sheets. Such arrivals cannot be explained without assuming pronounced transverse isotropy and modelling with full-wave synthetic seismograms. They may be important for exploration seismology as they provide additional signals, with different characteristics that may be used to examine the internal structure of a zone of interest. Moreover, if wrongly identified, they could lead to (possibly severe) misinterpretations of subsurface structure. Azimuthal anisotropy of vertical cracks, with crack density $\varepsilon = 0.014$ and strike N203°E in the top 870 m, must also be included to reproduce the sagittal to transverse coupling of the three-component recordings.

The data show anomalies in the relative amplitudes of three-component seismograms that are probably caused by variations of natural directivity (ND) near the positions of the shear-wave source locations. The effects of ND could have serious implications for the detailed interpretation of all experiments involving near-surface shear-wave sources.

REFERENCES

Brodov. L.Y., Evstifeyev, V.I., Karus, E.V. and Kulichikhina, T.N., 1984, Some results of the experimental study of sedimentary rocks using different types of waves: Geophys. J. Roy. Astr. Soc. 76, 191-200.

_____, Zatsepin, S.V. and Tertychniyi, V.V., 1992, Kinematic inversion of seismic data for determination of crack and pore structure in anisotropic reservoir rock: Presented at the 5th Internat. Workshop on Seismic Anisotropy, Banff, Abstr. 22.

Campden, D.A., Crampin, S., Majer, E.L. and McEvilly, T.V., 1990, Modelling the Geysers VSP: a progress report: The Leading Edge **9,** 8, 36-39.

Castagna, J.P., Batzle, M.L. and Eastwood, R.L., 1985, Relationships between compressional-wave and shear-wave velocities in clastic silicate rocks: Geophysics **50,** 57 I-58 1.

Crampin, S., 1981, A review of wave motion in anisotropic and cracked elastic-media: Wave Motion **3,** 343-39 1.

_____, 1987, Geological and industrial implications of extensive-dilatancy anisotropy: Nature **328,** 49 I-496.

_____, 1989, Suggestions for a consistent terminology for seismic anisotropy: Geophys. Prosp. 37, 753-770.

_____, 1993, Arguments for EDA: Can. J. Expl. Geophys. 29, 18-30.

_____ and Lovell. J.H., 199 1, A decade of shear-wave splitting in the Earth's crust: what does it mean? what use can we make of it'? and what should we do next?: Geophys. J. Internat. **107,** 387-407.

Gardener, G.H.F., Gardener, L.W. and Gregory, A.R., 1974, Formation velocity and density - the diagnostic basics for stratigraphic traps: Geophysics 39, 770-780.

Jolly, R.N., 1956, Investigation of shear waves: Geophysics **21,** 905-938.

Kaarsberg, E.A., 1968, Elasticity studies of isotropic and anisotropic rock samples: Trans. Soc. Min. Eng. **241,** 470-475.

Levin, F.K., 1979, Seismic velocities in transversely isotropic media: Geophysics **44,** 9 18-936.

MacBeth, C., Wild, P., Crampin, S. and Brodov, L.Y., 1993, Optimal acquisition geometry for recording shear-wave anisotropy: Can. J. Expl. Geophys. 29,132- 139.

Majer, E.L., McEvilly, T.V., Eastwood, F.S. and Myer, L.R., 1988, Fracture detection using P-wave and S-wave vertical seismic profiling at the Geysers: Geophysics **53,** 76-84.

Musgrave, M.J.P., 1954, On the propagation of elastic waves in aeolotropic media II. Media of hexagonal symmetry: Proc. Roy. Soc. London A226, 356-366.

Nalivkin, D.V., 1973, Geology of the U.S.S.R.: Oliver and Boyd, Edinburgh.

Postma, G.W., 1955, Wave propagation in a stratified medium: Geophysics **20,** 780-806.

Puzirev, N.N. and Brodov, L.Y., 1969, Efficient SH-wave generation: Geol. Geofiz. 5, 8 I-88.

,Trigubov, A.V. and Brodov, L.Y., 1985, Seismic prospecting methods in shear and converted waves (in Russian): Nedra, Moscow.

Riznichenko, Y.V., 1949, On seismic quasi-anisotropy (in Russian): Izv. Akad. Nauk SSSR, Ser. Geogr. Geofiz. **13,** 5 18-544.

Taylor, D.B., 1990, ANISEIS manual: version 4.5: Applied Geophysical Software Inc., Houston.

Uhrig, L.F. and Van Melle, F.A., 1955, Velocity anisotropy in stratified media: Geophysics **20,** 774-779.

White, J.E., 1982, Computed waveforms in transversely isotropic media: Geophysics **47,** 77 l-783.